Norrishite, $K(Mn_2^{3+}Li)Si_4O_{10}(O)_2$, an oxymica associated with sugilite from the Wessels Mine, South Africa: Crystal chemistry and ^{40}Ar-^{39}Ar dating

EDWIN GNOS,[1,*] THOMAS ARMBRUSTER,[2] AND IGOR M. VILLA[1]

[1]Intitut für Geologie, Universität Bern, Baltzerstrasse 1, CH-3012 Bern, Switzerland
[2]Laboratorium für Chemische und Mineralogische Kristallographie, Universität Bern, Freiestrasse 3, CH-3012 Bern, Switzerland

ABSTRACT

Norrishite, $K(Mn_2^{3+}Li)Si_4O_{10}(O)_2$, an OH-free mica, is found in a silicate-rich sample from the Wessels mine, Kalahari manganese field, South Africa. The mineral forms centimeter-sized black aggregates in dark-purple sugilite, and is associated with kornite and Mn-rich pectolite.

Single-crystal X-ray data, collected on norrishite of end-member composition, yielded a monoclinic $C2/m$ lattice with $a = 5.291(2)$, $b = 8.904(2)$, $c = 10.049(4)$ Å, $\beta = 98.15(5)°$, $V = 920.6$ Å³, and $Z = 2$, characteristic of the $1M$ polytype.

^{40}Ar-^{39}Ar analyses on a gem-quality sugilite yielded an age of 1048.1 ± 5.9 Ma interpreted as a mineral crystallization age that dates the main hydrothermal event that led to enrichment of the Mn ore. The norrishite age data are more complex and suggest a crystallization age ≈1010 Ma and a subsequent alteration at ca. 850 Ma. The age results obtained suggest that the hydrothermal activity is related to the collision and tectonism affecting the edges of the Kalahari craton, and show that sugilite, and probably also unaltered norrishite, are suitable for dating metamorphism.

INTRODUCTION

Oxidized Mn deposits of hydrothermal origin are alkali-rich (Na, K, and Li), and commonly contain appreciable amounts of Ba, Sr, and Ca (and lesser Cu, Co, Pb, As; Ashley 1986). This leads to characteristic oxidized assemblages associated with more reduced parageneses. Oxidized assemblages of different metamorphic grade are known from Mn deposits in Australia (Ashley 1986; Kawachi et al. 1994), Italy (Dal Piaz et al. 1979; Griffin and Mottana 1982; Lucchetti et al. 1988), Japan (Nambu et al. 1969), Russia (Kalinin 1980), and India (Dasgupta et al. 1991; Roy 1971). Norrishite, $K(Mn_2^{3+}Li)Si_4O_{10}(O)_2$, has previously been reported only from the oxidized lower-greenschist facies stratiform manganese deposit of submarine exhalative origin of the Hoskins mine in New South Wales, Australia (Ashley 1986; Eggleton and Ashley 1989; Tyrna and Guggenheim 1991; Hawthorne et al. 1995). There, the mineral occurs in quartz-free and quartz-bearing assemblages associated with Mn-rich alkali pyroxenes, Mn-rich alkali amphiboles, manganoan pectolite, braunite, carbonates, feldspar, and less commonly with sugilite (Ashley 1986; Eggleton and Ashley 1989; Hawthorne et al. 1995). Tyrna and Guggenheim (1991) refined the crystal structure of the Australian type-locality norrishite and described it as trioctahedral "oxymica," where the site normally occupied by OH⁻ is occupied by O²⁻. A similar replacement of OH⁻ by O²⁻ may also occur in other micas like oxybiotite (e.g., Ohata et al. 1982).

During a survey on Mn-rich minerals occurring in pockets in the Wessels mine, Kalahari Mn field, South Africa (e.g., Cairncross et al. 1997), we noted a sample of dark purple sugilite containing cm-sized, black patches of a lustreous, biotite-looking material subsequently identified as norrishite. These materials were evaluated to determine whether they could provide reliable ^{39}Ar-^{40}Ar age estimates of the hydrothermal activity related to the Mn ore-forming event.

GEOLOGIC SETTING AND SAMPLE DESCRIPTION

Manganese is mined in the Kalahari Mn field from hydrothermal enrichments in stratabound deposits, which formed at approximately 2100 Ma (Dixon 1989; Söhnge 1977). The Mn deposits belong to the Hotazel member of the Griqualand West Sequence, and occur in association with cherts (jasper) and mafic volcanic rocks (pillow lavas and hyaloclastic rocks). Kutnahorite-bearing pisolitic hematite lutites and braunite lutites are generally described as the protolith ore. Manganese enrichment occurred in the northwestern part of the Mn field due to metamorphic recrystallization caused by hydrothermal circulation along faults. Conditions during metamorphism were in the range of 270–420 °C at 0.2–1.0 kbar (Dixon 1989; Gutzmer and Beukes 1998). The Mn-rich recrystallized ore consists mainly of hausmannite, bixbyite, braunite, and manganite. Within the ore-rich zones are silicate-rich pockets that are well known for pink to dark purple sugilite of gem quality (Armbruster and Oberhänsli 1988; Dixon 1989; Dunn et al. 1980). Our sample was collected from the sugilite occurrences located in the lower Mn-ore layer at Wessels mine.

This norrishite-bearing specimen N2 (Fig. 1) is sugilite-rich and contains centimeter-sized patches of black mica. The macroscopic appearance is like biotite. In thin section, this mica was identified as norrishite by its bright lemon-yellow to brownish-yellow pleochroism, and its optically positive character. The mica occurs in a matrix of sugilite, KNa_2
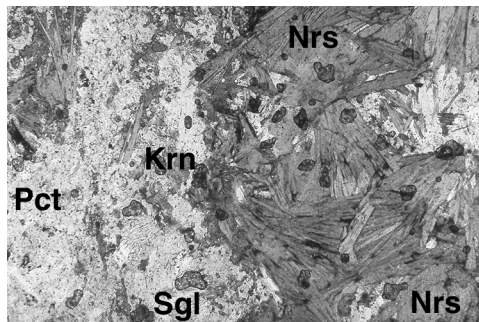
FIGURE 1. Thin section photomicrograph showing norrishite (Nrs) associated with kornite (Krn), sugilite (Sgl), and Mn-rich pectolite (Pct). Sample N2, base of picture 2.4 mm.

$(Fe^{3+},Mn^{3+})_3(Li,Al,Fe^{3+})_3Si_{12}O_{30}$; pectolite, $Na(Ca,Mn)_2Si_3O_8$ (OH); and pink to red-pleochroic short-prismatic kornite, $(K,Na)(Na,Li)_2(Mg,Mn^{3+},Fe^{3+},Li)[Si_8O_{22}](OH)_2$ (Armbruster et al. 1993). Small grains of strontianite and orange-brown hennomartinite, $Sr_2Mn_2^{3+}[Si_2O_7](OH)_2$ (Armbruster et al. 1993), occur as accessories. Although sugilite is macroscopically bright purple in color, it is colorless in thin section (like most ring silicates), and typically forms poikiloblasts overgrowing pectolite and kornite. In sample N8, which was used for age dating, sugilite forms half-centimeter sized inclusion-free crystals and is associated with Mn-rich pectolite.

MINERAL CHEMISTRY

Mineral compositions were determined by electron probe microanalysis (Cameca SX-50) using beam conditions of 15 kV and 20 nA, an enlarged spot size of about 10 μm, and wavelength-dispersive spectroscopy. Data for Ti, F, and Cl were collected for 30 seconds on peak and background, and all other elements for 20 seconds.

Norrishite chemistry shows very little deviation from the ideal end-member, with traces of Al, Mg, and Na present (Table 1). Fluorine and Cl are at the detection limit and the mineral is completely free of Fe. The Li content was confirmed by single-crystal structure refinement. Stoichiometry and bond strength requirements indicate that norrishite is an "oxymica" without OH. Lithium (Li = 6 cations-Ti-Cr-Fe-Mn-Mg-Ca) and O (2-Cl-F) were subsequently calculated by stoichiometry (Table 1). Manganese-rich pectolite contains 6.5–19.1 wt% MnO, and two Mn-rich pectolites with different Mn contents (Table 1) seem to coexist in sample N2. Chlorine and F are near the detection limit, whereas Ba, Sr, and Pb were not detected in qualitative scans. The red pleochroic alkali amphibole in the norrishite sample is kornite and contains Li (Armbruster and Oberhänsli 1988), 0–2.2 wt% Fe_2O_3, and up to 2.5 wt% CaO. The Li content of kornite was calculated as Li = 5 cations-Al-Ti-Cr-Fe-Mn-Mg-Ca. Sugilite in the norrishite sample contains 7.8–10.4 wt% Fe_2O_3 with a typical K:Na value in the formula unit of 1:2. The presence of Fe^{3+} is considered the cause of the lilac color of the Kalahari sugilite (Armbruster and Oberhänsli 1988; Dixon 1989; Fritsch and Shigley 1994; Taggart et al. 1994). The inclusion-free, gem-quality sugilite in sample N8 used for the ^{40}Ar-^{39}Ar analysis contains 12.8–13.9 wt% Fe_2O_3 and approximately 4.7–4.8 wt% K_2O. The Li-content in sugilite was calculated as Li = 5 cations-Al-Ti-Cr-Fe-Mn-Ca.

SINGLE-CRYSTAL X-RAY DATA COLLECTION AND REFINEMENT

A lustrous black flaky, unbent norrishite crystal (0.150 × 0.150 × 0.040 mm³) was selected for structural study with an ENRAF NONIUS CAD4 single-crystal X-ray diffractometer, using a graphite monochromator and MoKa X-radiation at room temperature (293 K). Cell dimensions were refined from the angular settings of reflections with 8 < θ < 19° yielding $C2/m$ monoclinic symmetry with a = 5.291(2), b = 8.904(2), c = 10.049(4) Å, β = 98.15(5)°, V = 920.6 Å³. The crystal did not show any obvious indication of twinning or polymorphism in its X-ray diffraction (XRD) pattern, but all reflections were strongly smeared out (>7°) along the omega-direction.

Diffraction data were collected up to θ = 30° and corrected for background and Lorenz polarization effects using the SDP program system (Enraf Nonius 1983). An empirical absorption correction using the ψ-scan technique was applied. Structure solution and refinement were performed with neutral-atom scattering factors and the programs SHELXS-97 and SHELXL-97 (Sheldrick 1997). The refinement converged at R1 = 8.7% with 574 F_o > 4s (F_o) and 56 parameters. Atomic coordinates and displacements were not significantly different from those given by Tyrna and Guggenheim (1991) and are therefore not tabulated. The structural refinement confirmed the end-member formula $K(Mn_2^{3+}Li)Si_4O_{10}(O)_2$ (Table 1, N2norx) and complete Li/Mn ordering, as already shown by Tyrna and Guggenheim (1991).

^{40}Ar-^{39}Ar DATING

Potassium-bearing Mn oxides were recently used for dating supergene deposits in a tropical climate (e.g., Vasconcelos et al. 1995). Although hydrothermal Mn deposits commonly contain K-bearing Mn minerals, few attempts have been made to use such minerals for dating the metamorphism of the Mn ore.

Micas rich in K are normally suitable for ^{40}Ar-^{39}Ar dating. Norrishite contains approximately 10 wt% K_2O (Table 1). Moreover, it is OH-free, which renders gas purification easy. We also selected a larger inclusion-free sugilite crystal from sample N8 that contains 4.5–5 wt% K_2O (Table 1) in order to test whether this mineral structure, which contains large cavities (Armbruster and Oberhänsli 1988), is suitable for Ar dating.

Norrishite and sugilite fragments were hand-picked from a small piece of crushed sample. Analytical techniques followed those of Villa et al. (2000), and results are listed in Table 2. Samples were measured long after ^{37}Ar from Ca had decayed, but it did not impact age estimates because the analyzed minerals contain almost no Ca (Table 1). MMhb1 with a known age of 520.4 Ma was used as neutron flux monitor (Samson and Alexander 1987).

DISCUSSION

Crystal chemistry

Tyrna and Guggenheim (1991) suggested that the lack of Fe in norrishite is caused by the Fe-poor bulk chemistry of the host rock and that an Fe^{3+} equivalent may be synthesized, as the ionic radii of Fe^{3+} and Mn^{3+} are equal. Although norrishite in our sample from the Wessels mine occurs in association with Fe^{3+}-bearing sugilite showing variable Fe_2O_3 contents (Table 1), the mica is absolutely Fe free. Our structure refinement

TABLE 1. Chemical composition of norrishite and associated minerals

Sample	N2 nrs3	N2 nrs7	N2 nrs11	N2 nrs (n = 22) average	N2 sgl	N2 sgl	N2 krn18	N2 krn45	N2 pct21	N2 pct25	N8 sgl7	N8 pct17
SiO_2	53.54	53.13	52.81	52.70(50)	70.15	71.44	56.29	55.53	52.55	54.34	68.83	52.92
TiO_2†	0.00	0.02	0.00	0.01(1)	0.01	0.04	0.03	0.00	0.01	0.02	0.00	0.00
Cr_2O_3†	0.00	0.00	0.00	0.00(0)	0.00	0.00	0.00	0.00	0.00	0.00	0.00	0.00
Al_2O_3†	0.01	0.12	0.02	0.07(5)	1.38	1.69	0.02	0.09	0.00	0.02	0.18	0.01
Fe_2O_3	0.00	0.00	0.00	0.00(0)	10.28	9.51	0.00	2.12	0.00	0.00	13.47	0.00
FeO†	0.00	0.00	0.00	0.00(0)	0.00	0.00	0.00	0.00	0.00	0.08	0.00	0.29
Mn_2O_3	31.40	31.27	31.67	31.17(25)	2.13	2.78	19.04	16.80	18.86	6.74	1.05	14.81
MgO†	0.05	0.16	0.03	0.12(6)	0.01	0.02	8.55	8.11	0.14	0.20	0.09	0.09
CaO†	0.00	0.04	0.01	0.02(2)	0.68	0.26	0.13	1.45	17.60	27.19	0.00	20.08
Na_2O†	0.02	0.02	0.01	0.03(2)	5.94	6.07	8.22	8.55	8.56	8.94	5.90	8.58
K_2O	10.60	10.14	10.44	10.50(16)	4.65	4.69	3.71	3.14	0.01	0.14	4.76	0.00
Li_2O	3.31*	3.35*	3.16*	3.19(10)*	4.06*	4.11*	1.43*	1.21*	–	–	4.07*	–
F†	0.00	0.00	0.03	0.01(1)	–	–	0.00	0.00	0.13	0.00	–	0.00
Cl†	0.00	0.01	0.00	0.00(2)	–	–	0.00	0.00	0.01	0.00	–	0.01
H_2O	–	–	–	–	–	–	3.29*	3.26*	2.54*	2.68*	–	*2.60
O_2	1.78*	1.77*	1.76*	1.76(2)*	–	–	–	–	–	–	–	–
Total	100.71	100.03	99.94	99.79(46)	99.29	100.61	100.71	100.26	100.41	100.35	98.35	99.39
				Formula proportions								
Si	7.993	7.995	7.947	7.948(34)	12'	12'	8'	8'	6.051	6.087	12'	6.106
Ti	0.000	0.000	0.000	0.001(2)	0.001	0.004	0.003	0.000	0.001	0.002	0.037	0.000
Cr	0.000	0.000	0.000	0.000(0)	0.000	0.000	0.000	0.000	0.000	0.000	0.000	0.000
Al	0.001	0.022	0.004	0.012(9)	0.278	0.334	0.003	0.015	0.000	0.003	0.000	0.002
Fe^{3+}	0.000	0.000	0.000	0.000(0)	1.323	0.000	0.000	0.000	0.000	0.000	1.767	0.000
Fe^{2+}	0.000	0.000	0.000	0.000(0)	0.000	1.203	0.000	0.231	0.000	0.008	0.000	0.028
Mn	3.971	3.986	4.037	3.980(26)	0.309	0.396	2.292	2.051	1.839	0.640	0.156	1.448
Mg	0.010	0.000	0.006	0.028(14)	0.003	0.005	1.810	1.740	0.025	0.034	0.024	0.015
Ca	0.000	0.006	0.001	0.000(0)	0.125	0.046	0.020	0.223	2.172	3.264	0.001	2.483
Na	0.006	0.005	0.001	0.006(4)	1.970	1.978	2.264	2.389	1.911	1.943	1.995	1.919
K	2.019	1.946	2.004	2.022(29)	1.015	1.005	0.672	0.577	0.001	0.021	1.058	0.000
Li	2.021*	1.944*	*2.009	1.930(58)*	2.961*	3.013*	0.871*	0.739*	–	–	2.985*	–
F	0.000	0.000	0.016	0.012(21)	–	–	†	†	0.047	0.000	–	0.000
Cl	0.000	0.003	0.000	0.002(2)	–	–	†	†	0.002	0.000	–	0.002
O	1.996*	1.997*	*1.984	1.986(21)*	–	–	–	–	–	–	–	–
OH	–	–	–	–	–	–	2.000*	2.000*	1.951*	2.000*	–	1.998*

Notes: The following natural and synthetic standards, lines, and spectrometer crystals were used (generally $K\alpha$ lines): tephroite, Mn (LiF); orthoclase, K (PET) and Si (TAP); anorthite, Al (TAP) and Ca(PET); spinel, Mg (TAP); almandine, Fe (LiF); albite, Na (TAP); ilmenite, Ti (PET); fluorphlogopite, F (TAP); scapolite, Cl (PET). Norrishite analyses were normalized 14 cations and a total charge of 46, pectolite to 12 cations and 2 OH and a total charge of 34, all other minerals to a fixed value of the element marked with a prime.
nrs = norrishite; sgl = sugilite; krn = kornite; pct = pectolite.
* Calculated value.
† Listed values = 0.04 are at or below the detection limit.

shows that the asymmetric displacement of the M2 site in norrishite caused by the presence of O^{2-} instead of OH^-, and the octahedral distortion caused by the size and charge difference of the cations on M1 and M2, produce the environment preferentially occupied by the Jahn-Teller ion Mn^{3+}, which contains an anisotropic electron configuration with tetragonal symmetry. Because Fe^{3+} would be available in the rock, the strongly distorted octahedral site in norrishite seems to be the main reason why the mineral is Fe-free. In addition to K, Na is also abundant in the norrishite rock, and one could expect that an oxymica with the formula $Na(Mn_2^{3+}Li)Si_4O_{12}$ would form. However, the much smaller ionic radius of Na (1.12 Å) compared with K (1.51 Å) seems to preclude this. It is thus expected that norrishite shows only very limited solid solution with other silicate micas.

The octahedral sheet charge of norrishite containing 4 Mn^{3+} and 2 Li per formula unit (pfu) is 14, in contrast to common micas where it is 12. This difference implies that the OH group is replaced by divalent anions for charge balance and that a tetrahedral replacement of Si by Al is hardly possible because this would make necessary one additional negative charge per formula unit.

Metamorphism

Norrishite at its type locality occurs in a greenschist-facies, oxidized Mn ore (450–500 °C; Ashley 1986). Pressure-temperature estimates for the Wessels deposit are lower [270–420 °C at 0.2–1.0 kbar (Dixon 1989; Gutzmer and Beukes 1998)]. At both localities, the assemblage containing norrishite + kornite + Mn-rich pectolite is similar. Namansilite ($NaMn^{3+}Si_2O_6$) ± quartz occurs at the Hoskins mine, whereas Fe^{3+}-bearing sugilite occurs only at the Wessels mine. Recently sugilite was also reported in other assemblages from the Hoskins Mine. The occurrence of similar assemblages at different metamorphic grade suggests that the highly oxidizing conditions and availability of Li play a major role in stabilizing the norrishite-bearing assemblages.

Crystallization age

The age spectrum obtained for the hand-picked norrishite concentrate is irregular, whereas the sugilite age spectrum shows a well defined plateau (Figs. 2a and 2b). For the sugilite, the weighted average for steps 3–8, which comprises 99.7% of the ^{39}Ar released, yields an age of 1048.1 ± 5.9 Ma (Fig. 2a). Al-

TABLE 2. ^{40}Ar- ^{39}Ar data of norrishite and sugilite

Step	T (°C)	^{40}Ar tot. (mL)	^{40}Ar sig.	^{40}Ar*	^{39}Ar	^{39}Ar sig.	%	^{38}Ar	^{38}Ar sig.	^{38}Ar (Cl)	^{36}Ar
					Norrishite						
1	445	8.75E-10	1.80E-13	4.71E-10	7.65E-12	2.20E-13	0.360	3.62E-12	3.00E-13	3.28E-12	1.37E-12
2	492	4.70E-10	3.90E-13	5.32E-10	6.27E-12	1.90E-13	0.294	2.37E-13	1.90E-13	2.01E-13	−2.12E-13
3	546	8.66E-10	5.40E-13	9.51E-10	9.75E-12	2.00E-13	0.458	2.08E-13	3.40E-13	1.49E-13	−2.88E-13
4	592	1.73E-09	4.20E-13	1.57E-09	1.49E-11	2.90E-13	0.701	4.32E-12	2.90E-13	1.49E-13	5.34E-13
5	643	5.09E-09	4.00E-13	5.00E-09	5.16E-11	2.20E-13	2.424	1.62E-12	1.90E-13	9.96E-13	3.73E-13
6	686	1.30E-08	1.30E-12	1.31E-08	1.22E-10	2.00E-13	5.731	8.53E-13	2.80E-13	5.41E-14	−2.10E-13
7	738	1.74E-08	1.60E-12	1.76E-08	1.61E-10	2.80E-13	7.573	2.43E-12	2.00E-13	6.20E-13	−4.63E-13
8	790	3.29E-08	2.20E-12	3.27E-08	3.03E-10	3.80E-13	14.223	5.13E-12	2.70E-13	1.48E-12	5.05E-13
9	829	5.30E-08	3.70E-12	5.28E-08	4.84E-10	4.70E-13	22.732	7.20E-12	1.90E-13	1.37E-12	7.01E-13
10	864	7.20E-08	5.90E-12	7.19E-08	6.55E-10	6.50E-13	30.755	9.81E-12	2.50E-13	2.06E-12	2.60E-13
11	910	2.65E-08	1.60E-12	2.65E-08	2.40E-10	3.10E-13	11.279	4.12E-12	3.00E-13	1.31E-12	−3.29E-14
12	969	5.05E-09	8.10E-13	4.83E-09	4.74E-11	2.40E-13	2.229	8.67E-13	1.60E-13	1.71E-12	7.79E-13
13	1083	3.13E-09	8.30E-13	3.16E-09	2.79E-11	2.30E-13	1.313	-7.27E-14	-3.40E-13	3.86E-14	−1.20E-13
	Total			2.31E-07	2.13E-09					1.19E-11	
	Total/g			4.44E-05	4.10E-06						
	K (g/g)				8.51E-02			Cl (g/g) =		1.09E-04	
	J = 0.00688										
	Wt = 0.00052g										
					Sugilite						
1	505	1.67E-09	4.30E-13	5.03E-11	2.47E-12	1.50E-13	0.104	8.16E-12	1.70E-13	7.11E-12	5.48E-12
2	609	6.14E-10	1.50E-13	2.95E-10	5.82E-12	2.10E-13	0.245	2.74E-12	1.70E-13	2.47E-12	1.07E-12
3	721	3.05E-08	3.10E-12	2.98E-08	2.60E-10	2.80E-13	10.939	7.17E-12	1.90E-13	3.70E-12	2.26E-12
4	797	4.75E-08	6.30E-13	4.70E-08	4.09E-10	4.10E-13	17.180	6.41E-12	2.20E-13	1.32E-12	1.48E-12
5	913	1.25E-07	1.40E-11	1.24E-07	1.07E-09	9.80E-13	45.149	2.00E-11	2.30E-13	7.00E-12	1.91E-12
6	1016	2.76E-08	2.40E-12	2.72E-08	2.38E-10	2.90E-13	9.982	3.65E-12	1.80E-13	5.93E-13	1.40E-12
7	1114	8.92E-09	5.10E-13	8.79E-09	7.65E-11	1.60E-13	3.212	1.09E-12	1.60E-13	1.11E-13	4.37E-13
8	1208	1.22E-08	7.40E-13	1.20E-08	1.07E-10	2.60E-13	4.491	1.19E-12	3.20E-13	1.91E-14	6.81E-13
9	1460	2.38E-08	2.20E-12	2.37E-08	2.07E-10	3.20E-13	8.697	3.67E-12	1.90E-13	1.14E-12	5.15E-13
	Total			2.73E-07	2.38E-09					2.35E-11	
	Tot/g			2.10E-04	1.83E-06						
	K (g/g)				3.81E-02			Cl(g/g) =		8.63E-05	
	J = 0.00688										
	Wt = 0.0013g										

Note: tot. = total; sig. = one sigma standard deviation; wt = weight.

though it is conceivable that cyclosilicates are affected by excess Ar, we believe two reasons argue against this possibility. (1) Isochron calculations show high mean-sum weighted deviate (MSWD) values, but invariably atmospheric initial Ar compositions over an about 700 °C degassing interval; the Ar release shows no strong degassing peak. (2) The most gas-rich step (no. 5, containing >45% of the total ^{39}Ar) has the highest step age, 1055 ± 1 Ma, which is contrary to the expected effect of excess Ar.

In order to interpret the discordant norrishite spectrum, we must focus on its mineralogy. Thin sections show fine-grained secondary minerals along the norrishite rims. These rims appear black under crossed polarizers (Fig. 1). How can we diagnose and deal with this alteration? The Cl/K values of norrishite show a negative correlation with step ages; this variation is compatible with incipient alteration of norrishite to Cl-richer clay minerals. A further effect of small clay particles is the recoil of ^{39}Ar, produced from the K that they contain, into the adjacent norrishite. We propose to view step 6 as the first degassing of norrishite sensu stricto (as opposed to the clay degassing in steps 1–5), so that step 6 gives a lowered age due to the release of recoil-implanted ^{39}Ar. Once this diagnosis has been made, how do we correct for it? A simple approach would be to select a discrete cutoff: all steps with Cl/K < 0.0023 are unaltered, and their average age is 1011 ± 7 Ma (MSWD 17).

However, calculating such an average may be illegitimate, as the high MSWD shows that the age spread is systematic and not noise. By taking into account the anticorrelation of Cl/K with age, one would expect the "true" age of the totally alteration-free reservoir to be slightly higher than the highest age of steps 8–11, i.e., >1019 ± 2 Ma. As the relative error on the Cl data is on the order of 100% for the Cl-poor steps below 700 °C, we cannot calculate a regression with any certainty. The value obtained when totally neglecting the uncertainties on the Cl/K ratios, ca. 1040 Ma, should be viewed as a semiquantitative indication only. In summary, according to the criteria chosen, one can assign the norrishite an age of at least 1010 Ma, which could become as high as 1040 Ma, very close to the sugilite age.

We must point out that the norrishite and the sugilite were not separated from the same sample and there are no independant estimates on how long the hydrothermal activity lasted. The robust evidence is that at least two episodes are recorded by our minerals: ca. 1050 Ma by sugilite and ca. 850 Ma by the clay-mineral alteration rims on norrishite.

Because the chemical composition, the cell parameters, and the crystal structure for both minerals are known (Armbruster and Oberhänsli 1988; Tyrna and Guggenheim 1991; this study), it is possible to calculate the ionic porosity for the two minerals as a proxy for the diffusion behavior of silicate minerals

TABLE 2.—*Extended*

^{39}Ar sig.	age (Ma)	age sig.	Cl/K
3.00E-13	637.39	100.00	0.09850554
−2.30E-13	829.49	86.00	0.007368725
−1.80E-13	927.05	43.00	0.00351925
2.30E-13	982.30	36.00	0.002301264
2.40E-13	924.97	8.70	0.004441085
−1.20E-13	995.34	2.40	0.000102013
−2.60E-13	1009.02	3.60	0.000884234
1.40E-13	1002.89	1.40	0.001120854
1.20E-13	1010.36	0.91	0.000649591
2.00E-13	1015.23	1.00	0.000724921
−1.90E-13	1018.78	1.90	0.001250226
2.10E-13	957.75	9.90	0.000831418
−1.30E-13	1038.10	11.00	0.000317708
			0.001281465
1.50E-13	236.29	200.00	0.661969303
2.80E-13	539.04	130.00	0.097647613
2.50E-13	1048.33	2.20	0.003264842
3.10E-13	1051.35	1.70	0.000741632
1.60E-13	1054.91	0.80	0.001498901
1.10E-13	1047.22	1.30	0.000573618
1.90E-13	1051.28	5.40	0.000335208
1.90E-13	1033.43	4.10	4.09861E-05
1.40E-13	1047.23	1.80	0.001269543
			0.002267005
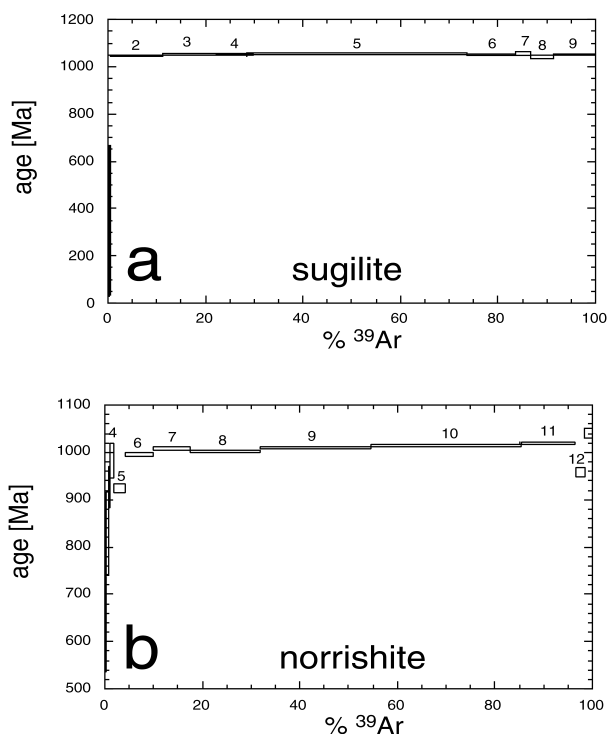
FIGURE 2. ^{39}Ar-^{40}Ar and and Ca/K spectra for (**a**) sugilite and (**b**) norrishite.

(Fortier and Giletti 1989; Dahl 1996). As expected from its crystal structure, the ionic porosity of 33.9% calculated for norrishite is low compared with common micas (e.g., Dahl 1996) and diffusive Ar loss will thus be lower. This result implies that the closing temperature for norrishite lies above that of common micas (i.e., >~400 °C), yet temperatures above 420 °C were not reached during the hydrothermal activity (Dixon 1989; Gutzmer and Beukes 1998). The calculated ionic porosity for sugilite is 39.1%, which is in the range of amphiboles or micas (Fortier and Giletti 1989). Thus the ionic porosity data also suggest that both norrishite and sugilite represent the age of the crystallization of the two minerals during one or several closely spaced hydrothermal events.

It is interesting to note that the ages obtained for the hydrothermal activity overlap with the time range of magmatic emplacement in the Namaqua area (Barton 1983a, 1983b), which is constrained by U-Pb and Rb-Sr methods at 1020–1085 Ma. Robb et al. (1998) also suggested an orogenic episode involving crustal thickening and magmatism at 1060–1030 Ma (U-Pb SHRIMP dating on zircon in orthogneisses) that was responsible for, and coeval with, the peak of high-grade low-pressure metamorphism. Mica cooling ages for the Gariep belt, Namaqua Province, range from 976 to 1006 Ma (Renne et al. 1990; Frimmel and Frank 1998). The hydrothermal activity causing the local enrichment of the Mn ore to economic con-

centrations thus seems directly related to collisional tectonics and probably occurred during the peak of metamorphism along the edges of the Kalahari craton.

REFERENCES CITED

Armbruster, T. and Oberhänsli, R. (1988) Crystal chemistry of double-ring silicates: Structures of sugilite and brannockite. American Mineralogist, 73, 595–600.

Armbruster, T., Oberhänsli, R., Bermanec, V., and Dixon, R. (1993) Hennomartinite and kornite, two new Mn^{3+} rich silicates from the Wessels Mine, Kalahari, South Africa. Schweizerische Mineralogische und Petrographische Mitteilungen, 73, 349–355.

Ashley, P.M. (1986) An unusual manganese silicate occurrence at the Hoskins mine, Grenfell district, New South Wales. Australian Journal of Earth Science, 33, 443–456.

Barton, E.S. (1983a) Reconnaissance isotopic investigation in the Namaqua mobile belt and implications for Proterozoic crustal evolution—Uptington Geotraverse. Geological Society of South Africa Special Publication, 10, 173–191.

———(1983b) Reconnaissance isotopic investigation in the Namaqua mobile belt and implications fro Proterozoic crustal evolution—Namaqualand Geotraverse. Geological Society of South Africa Special Publication, 10, 45–66.

Cairncross, B., Beukes, N., and Gutzmer, J. (1997) The manganese adventure. The South African manganese fields. 236 p. The Associated Ore & Metal Corporation Limited, Johannesburg, South Africa.

Dahl, P.S. (1996) The crystal-chemical basis for Ar retention in micas: inference from interlayer partitioning and implications for geochronology. Contributions to Mineralogy and Petrology, 123, 22–39.

Dal Piaz, G.V., Di Battistini, G., Kienast, J.R., and Venturelli, G. (1979) The manganiferous deposits of the Valsesia-Valtournanche area. Memorie degli Istituti di Geologia e Mineralogia dell'Università di Padova, 32, 4–22.

Dasgupta, S., Chakraborti, S., Sengupta, P., Bhattacharya, P.K., Banerjeee, H., Roy, S., and Fukuoka, M. (1991) Manganese-rich minerals of the pumpellyite group from the Precambrian Sausar Group, India. American Mineralogist, 76, 241–

245.

Dixon, R.D. (1989) Sugilite and associated metamorphic silicate minerals from Wessels Mine, Kalahari manganese fied. Bulletin of the Geological Survey of South Africa, 93, 1–47.

Dunn, P.J., Brummer, J.J., and Belsky, H. (1980) Sugilite, a second occurrence: Wessels Mine, Kalahari manganese field, Republic of South Africa. Canadian Mineralogist, 18, 37–39.

Eggleton, R.A. and Ashley, P.M. (1989) Norrishite, a new manganese mica, K(Mn$_2^{3+}$Li)Si$_4$)O$_{12}$ from the Hoskins mine, New South Wales, Australia. American Mineralogist, 74, 1360–1367.

Enraf Nonius (1983) Structure determination package (SDP). Enraf-Nonius, Delft, The Netherlands.

Fortier, S.M. and Giletti, B.J. (1989) An empirical model for predicting diffusion coefficients in silicate minerals. Science, 245, 1481–1484.

Frimmel, H.E. and Frank, W. (1998) Neoproterozoic tectono-thermal evolution of the Gariep Belt and its basement, Namibia and South Africa. Precambrian Research, 90, 1–28.

Fritsch, E. and Shigley, J.E. (1994) Causes of the purple and pink colours of manganoan sugilites from the Wessels mine, South Africa. Mineralogical Magazine, 58, 681–685.

Griffin, W.L. and Mottana, A. (1982) Crystal chemistry of clinopyroxenes from the St. Marcel manganese deposit, Val d'Aosta, Italy. American Mineralogist, 67, 568–586.

Gutzmer, J. and Beukes, N.J. (1998) The manganese formation of the Neoproterozoic Penganga Group, India-revision of an enigma. Economic Geology, 93, 1091–1102.

Hawthorne, F.C., Oberti, R., Cannilo, E., Sardone, N., Zanetti, A., Grice, J.D., and Ashley, P.M. (1995) A new anhydrous amphibole from the Hoskins mine, Grenfall, New South Wales, Australia: description and crystal structure of ungarettite, NaNa$_2$(Mn$_2^{2+}$Mn$_3^{3+}$)Si$_8$O$_{22}$O$_2$. American Mineralogist, 80, 165–172.

Kalinin, V.V. (1980) Dzhezdy manganese deposit, Khazakhstan, USSR. In I. Varentsov, M. and G. Grasselly, Eds., Geology and geochemistry of manganese, vol. 2: Manganese deposits on continents, 2, p. 467–480. E. Schweizerbart'sche Verlagsbuchhandlung, Stuttgart.

Kawachi, Y., Ashley, P.M., Vince, D., and Goodman, M. (1994) Sugilite in mangane silicate rocks from the Hoskins mine and Woods mine, New South Wales, Australia. Mineralogical Magazine, 58, 671–677.

Lucchetti, G., Cortesogno, L., and Palenzona, A. (1988) Low-temperature metamorphic mineral assemblages in Mn-Fe ores from Cerchiara mine (northern Appennine, Italy). Neues Jahrbuch für Mineralogie Monatshefte, 8, 367–383.

Nambu, M., Tanida, K., and Kitamura, T. (1969) Kôzulite, a new alkali amphibole, from the Tanohata mine, Iwate prefecture, Japan. Journal of the Japanese Association of Mineralogists, Petrologists and Economic Geologists, 62, 311–328.

Ohata, T., Takeda, H., and Tekéuchi, Y. (1982) Mica polytism: similarities in the crystal structures of coexisting 1M and 2M$_1$ oxybiotite. American Mineralogist, 67, 298–310.

Renne, P.R., Onstott, T.C., D'Agrella-Filho, M.S., Pacca, I.G., and Teixeira, W. (1990) ^{40}Ar/^{39}Ar dating of 1.0–1.1 Ga magnetization from the São Francisco and Kalahari cratons: tectonic implications for Pan-African and Brasiliano mobile belts. Earth Planetary Science Letters, 101, 349–366.

Robb, L.J., Armstrong, R.A., and Waters, D.J. (1998) Nature and duration of midcrustal granulite facies metamorphism and crustal growth; evidence from single zircon U-Pb geochronology in Namaqualand, South Africa. Information Circular—University of the Witwatersrand, Economic Geology Research Unit. 323, University of the Witwatersrand, Economic Geology Research Unit. Johannesburg, South Africa, 1–38.

Roy, S. (1971) Studies on manganese-bearing silicate minerals from metamorphosed manganese formations of India. II. Blanfordite, manganoan diopside, and brown manganiferous pyroxene. Mineralogical Magazine, 38, 32–42.

Samson, S.D. and Alexander, E.C. (1987) Calibration of the interlaboratory ^{40}Ar-^{39}Ar dating standard, MMhb-1. Isotope Geoscience, 7, 27–34.

Sheldrick, G.M. (1997) SHELX-97, program for crystal structure determination. University of Göttingen, Germany.

Söhnge, P.G. (1977) Timing aspects of the manganese deposits of the Northern Cape Province (South Africa). In D.D. Klemm and H.J. Schneider, Eds., Time and stratabound ore deposits, p. 115–122. Springer Verlag, Heidelberg.

Taggart, J., Foord, E.E., and Shigley, J.E. (1994) Chemical composition and structural formula of manganoan sugilite from the Wessels Mine, Republic of South Africa. Mineralogical Magazine, 58, 679–681.

Tyrna, P.L. and Guggenheim, S. (1991) The crystal structure of norrishite, KLiMn$_2^{3+}$Si$_4$O$_{12}$, and oxygen-rich mica. American Mineralogist, 76, 266–271.

Vasconcelos, P.M., Renne, P.R., Becker, T.A., and Wenk, H.-R. (1995) Mechanism and kinetics of atmospheric, rediogenic , and nucleogenic argon release from cryptomelane during ^{40}Ar-^{39}Ar analysis. Geochemica and Cosmochimica Acta, 59, 2057–2070.

Villa, I.M., Hermann, J., Müntener, O., and Trommsdorff, V. (2000) 39Ar–40Ar dating of multiply-zoned amphibole generations (Malenco, Italian Alps). Contributions to Mineralogy and Petrology, 140, 363–381.